Transport of Viable Bacteria by Dust Plumes in the Eastern Mediterranean

Yinon Rudich (yinon.rudich@weizmann.ac.il)
Weizmann Institute of Science https://orcid.org/0000-0003-3149-0201
Burak Adnan Erkorkmaz
https://orcid.org/0000-0002-4334-4298
Daniella Gat
Weizmann Institute of Science https://orcid.org/0000-0002-0595-4626

Article

Keywords:

Posted Date: March 3rd, 2022

DOI: https://doi.org/10.21203/rs.3.rs-1400821/v1

Version of Record: A version of this preprint was published at Communications Earth & Environment on February 6th, 2023. See the published version at https://doi.org/10.1038/s43247-023-00679-8.

Abstract

Atmospheric transport of viable microorganisms can affect the biodiversity and health of global ecosystems. However, the processes influencing the abundance, composition and viability of airborne bacterial communities remain understudied. Using qPCR and high-throughput amplicon sequencing of DNA and RNA extracted from aerosol samples representing varying dust sources in the Eastern Mediterranean in a size-resolved manner, we report comprehensive and quantitative evidence of the atmospheric transport of viable airborne bacterial communities. We found that the air masses associated with dust sources increased the diversity (by ~ 0.3–0.4 times), richness (by ~ 2.5–3.9 times) and concentration (by ~ 6–30 times) of viable airborne bacteria. Our results suggest that the composition and abundance of viable airborne bacterial communities depend on the aerosol source. We found that some of the viable taxa (2 604 of 6 143 unique ASVs) had significantly higher RNA abundance than DNA abundance. The viable taxa, most of them associated with coarse particles (961 of 1 433 ASVs), were more likely to readily survive once they settled in a new environment. We suggest that viable bacteria are transported as cell aggregates and/or attached to particles; thus, they may be protected and survive for 3–4 days under harsh atmospheric conditions. Taken together, our results indicate that the atmosphere is a significant dispersal pathway for viable bacteria.

Introduction

Windblown dust can carry microorganisms great distances, from tens to thousands of kilometers [1–6]. Airborne microbial communities transported along with dust from various sources may significantly affect aquatic, atmospheric, and terrestrial ecosystems once the dust settles [7–13]. Bacteria constitute the major fraction of microorganisms emitted to the atmosphere, and once airborne, they can serve as condensation and ice nuclei [14–16] and can participate in cloud water chemistry [17–19]; additionally, transported pathogens may impact ecosystems, agriculture and human health [13,20,21]. Airborne bacteria from different sources have been shown to carry distinct microbial communities [22–24]. Recent studies have suggested that the community composition and the structure of airborne microorganisms are strongly affected by seasonality [25,26], air-mass origin, PM_{10} concentration [3,4,6], meteorological conditions, aerosol chemical composition [27], and the size of the particles [6,28–30].

Viable microorganisms represent a functional potential to drive ecosystem processes, whereas dead cells indicate the loss of ecosystem functional potential. Thus, characterizing community structure along with viability is of great importance and has been a longstanding goal of microbial ecology [31–33].

Most recent studies of the airborne microbiome have applied high-throughput sequencing of the 16S rRNA gene [3–5] to characterize its phylogenetic and taxonomic diversity without discerning between live and dead cells. In contrast, direct sequencing of ribosomal RNA may provide information regarding the phylogeny and taxonomy of viable bacteria [34]. Comparative analysis of rRNA and rRNA-encoding genes has recently provided meaningful ecological insights into terrestrial and aquatic environments regarding

communities' interactions with the environment [35–39]. However, little is known about the functional capacity of microbial communities transported in the atmosphere, mostly due to technical limitations such as low concentrations of microorganisms, challenges in acquiring high-quality genetic material, and the lack of advanced molecular tools [40–42]. Although some studies have used next-generation sequencing and have revealed a viable community potentially influencing the cycling of organic compounds [43] and interfering with abiotic chemical processes [44] in the atmosphere and in cloud water sampled at a mountaintop research station, there are still knowledge gaps regarding changes in the composition and extent of viability of airborne communities during their aerial transport and exposure to harsh atmospheric conditions. From an ecological perspective, improving our knowledge of the aerial transport of viable bacterial communities is particularly important because the dispersal of viable microorganisms is a key process, along with selection, drift and speciation, controlling the patterns that drive the diversity, abundance, and composition of species in microbial communities [45] and thereby significantly affecting the maintenance of global biodiversity.

Global climate change is projected to increase heat and drying processes in the Eastern Mediterranean and Middle East regions, resulting in elevated particulate matter concentrations and intensified dust event occurrences, further underscoring the importance of studying the transport of viable microbial communities on both global and regional scales [46,47].

Here, we present the first comprehensive and comparative study investigating viable bacterial communities transported from different air-mass sources using 16S ribosomal DNA and RNA high-throughput amplicon sequencing and quantitative polymerase chain reaction (qPCR) of size-resolved particulate matter. To accomplish this, we assembled a wide collection of dust samples of different origins in a size-resolved manner. Using these tools, we attempted to quantify viable bacteria transported by dust from different sources; to describe the community composition of viable bacteria and compare these communities between the different sources and different particle size classes. Finally, we attempted to determine which airborne bacteria survive long-range atmospheric transport.

Materials And Methods

Sample collection

Atmospheric particulate matter with an aerodynamic diameter smaller than 10 μm (PM_{10}) was collected on quartz microfiber filters (Whatman Sigma-Aldrich, Saint Louis, MO, USA, 203 mm × 254 mm for backup stage, and Tisch Environmental, Inc., Cleves, OH, USA, TE-230-QZ Slotted Quartz Fiber for a five-stage high volume cascade impactor); all the filters were pre-baked at 450 °C for 5 h prior to sampling to rid them of all organic matter. Sampling was performed using a high-volume air sampler (Tisch Environmental, Inc., TE-6070X) at a flow rate of 67.96 m^3 hr^{-1} for six hours at a time. Operating blanks were obtained following the same procedure but were placed in the sampler for only 5 min of operation.

A five-stage high volume cascade impactor (Tisch Environmental, Inc., TE-235) was used to procure size segregated samples (<0.49 µm, 0.49-0.95 µm, 0.95-1.5 µm, 1.5-3.0 µm, 3.0-7.2 µm, 7.2-10.0 µm). All the samples were collected on the roof of a four-story building at the Weizmann Institute of Science, Rehovot, Israel (31.9070 N, 34.8102 E; 80 m amsl). Sampling was designed to capture particulate matter originating from various sources (*e.g.*, Sahara, Arabia, Syria) under varying concentrations (*i.e.*, low and high PM_{10}) [48]. To achieve this sampling design, we followed various atmospheric forecast platforms (https://www.windy.com/; https://forecast.uoa.gr/en/forecast-maps/dust/europe; and https://dust.aemet.es/forecast/nmmb-bsc-dust-forecast-sconc) to predict and prepare for upcoming dust storms. These predictions were verified by the online PM_{10} data of the Israeli Ministry of Environmental Protection database, Rehovot Air Monitoring station (https://www.svivaaqm.net/). At the end of each sampling event, the filters were cut using a sterile surgical scalpel and forceps and immediately submerged in RNA fixative solution (280 $g \cdot L^{-1}$ ammonium sulfate dissolved in 25 mM sodium sulfate solution with 10 mM EDTA, pH 5.2). The samples were kept at -20 °C until downstream processing. All prepared batches of the RNA fixative solution were poured into several sterile petri dishes in a biological hood and UV sterilized twice for 15 minutes each.

Particulate matter concentration data, backward trajectory analyses and dust column mass density maps

Particulate matter concentration data were obtained from the Rehovot Air Monitoring station, located approximately 1 km from our sampling site. This station is part of the Israeli Ministry of Environmental Protection network. PM_{10} concentration data were obtained in 5-minute time intervals and were used to calculate the mean concentration for each sampling period.

To identify the air-mass sources, back trajectories were calculated using the hybrid single-particle Lagrangian integrated trajectory model (HYSPLIT) [49,50] via the web interface (READY, http://ready.arl.noaa.gov/HYSPLIT_traj.php). Each back-trajectory was calculated for a 72 h duration at 3 different altitudes (0, 50 and 100 meters high). The results are presented in Table S1.

To identify the potential dust sources, time-averaged maps of dust column mass density (hourly 0.5° × 0.625°) reanalysis data were acquired from Modern-Era Retrospective analysis for Research and Applications (MERRA-2) for each sampling event. Each retrospective analysis consisted of time-averaged hourly frames (*i.e.*, maps of the given region) of dust column density maps for a period of 72 hours prior to the sampled event (including the sampling period) that were animated into short video clips for each sampling date (Movie S1-12). Analyses and visualizations used in this study were produced with the Giovanni online data system, developed and maintained by the NASA GES DISC [51].

Nucleic acid extraction and cDNA synthesis

DNA and RNA were coextracted from the filters using a PowerWater DNA isolation kit (Qiagen, Dresden, Germany) following the manufacturer's protocol, with the following adjustments. Filter pieces (1×12 cm) were removed from the RNA-preserving solution and placed into separate bead tubes. One milliliter of

PW1 solution was added to each tube, and the tubes were then vortexed horizontally for 5 min, followed by centrifugation at 2 700 *g* for 2 min. The supernatant from each bead tube was split into two aliquots and placed in 2 ml collection tubes. Then, we followed the manufacturer's protocol up to the last step (elution), which we repeated twice, using 50 µl of PW6 solution each time; the spin filter was soaked at room temperature for 5 min prior to centrifugation at 13 000 *g* for 1 min. A total of 100 µl of DNA/RNA solution per tube was obtained. Next, the DNA/RNA solution was split into two 50 µl aliquots. One of these aliquots was kept without further processing and was used in amplification and sequencing steps as a DNA sample.

The other 50 µl aliquot was treated with 1 µl DNase (DNase I, RNase-free, Thermo Fischer Scientific, Roskilde, Denmark) and incubated at 37 °C for 30 minutes to digest all the DNA. This reaction was repeated twice consecutively to remove any minute residues of DNA molecules in the sample. This aliquot was used for downstream reverse transcription and sequencing as an RNA sample.

cDNA was synthesized from the RNA extracts using a High-Capacity cDNA Reverse Transcription Kit (Applied Biosystems, Life Technologies, CA, USA) with random primers. To ensure that all DNA was digested in the previous step, we ran a control reaction for each sample to which no reverse transcriptase enzyme was added. These controls were treated according to the same steps as the true reaction samples, and no amplicons were evident after quantitative polymerase chain reaction (qPCR), indicating that all DNA was digested.

The concentrations of DNA and RNA in the sampled aerosols were determined using qPCR (StepOnePlus Real-Time PCR, Applied Biosystems, Life Technologies). qPCRs in this study were run using universal bacterial primers, 331F (TCCTACGGGAGGCAGCAGT) and 518R (ATTACCGCGGCTGCTGG) [52], targeting a fragment of the small subunit of the bacterial ribosome (SSU), also referred to as the 16S gene. qPCRs were performed in triplicate on each gDNA and cDNA sample, including reverse transcriptase negative control reactions and nontemplate controls. Each 20 µl reaction mixture was prepared as follows: 10 µl of SensiFAST SYBR mix (Bioline, London, UK), 1 µM of each primer, 4 µl of molecular grade H_2O, and 2 µl of template gDNA or cDNA. The following thermal cycling conditions were used for amplification: 3 min at 95 °C followed by 35 cycles of 5 s at 95 °C and 20 s at 60 °C. A logarithmic calibration curve of known concentrations of pNORM1 plasmid (designed by Christophe Merlin (LCPME, Nancy, France), synthesized by Eurofins Scientific) was used for quantification of the nucleic acids as previously described [3]. Total ribosomal DNA gene copies and RNA transcripts were normalized to the total volume of sampled air.

Amplification and sequencing

High-throughput amplicon sequencing (250×2 cycles) of 16S DNA and cDNA (rRNA transcripts that were converted to cDNA as described above) was conducted at the DNA Sequencing Facility (DNAS) at the University of Illinois at Chicago (UIC) using an Illumina MiSeq instrument. The target sequence was a segment of the V4 region in the 16S rRNA gene, amplified using tagged bacterial/archaeal primers as

follows: CS1_515F (ACACTGACGACATGGTTCTACAGTGCCAGCMGCCGCGGTAA) and CS2_806R (TACGGTAGCAGAGACTTGGTCTGGACTACHVGGGTWTCTAAT) [53].

Biostatistical microbiome data analysis

The sequencing data were analyzed using the R packages *DADA2* (version 1.16.0) [54] and *Phyloseq* (version 1.36.0) [55]. Sequences (*i.e.*, a total of 4 129 758) were quality-trimmed and filtered. Paired reads were merged, and chimeras were removed to produce amplicon sequence variants (ASVs). A total of 2 998 398 reads of bacterial 16S rRNA sequences (*i.e.*, DNA and RNA), including aerosol samples and blank filter controls (*i.e.*, 131 and 12 samples, respectively), were then assigned to 13 444 ASVs. The exact number of samples that were successfully sequenced and used for the biostatistical analyses for each air-mass source were in the northwest (NW, 6 and 18 for DNA and RNA, respectively), northeast (NE, 12 and 11), southwest (SW, 24 and 24) and southeast (SE, 12 and 12), summing to a total of 119 aerosol samples representing six different particle size classes in each sampling event.

Taxonomic classification of the obtained ASVs was performed using the SSURef SILVA database (v.138) [56]. The identification of contaminating sequences was conducted using the *decontam* package relying on sequence frequencies [57]. Identified contaminant sequences were subsequently removed from the dataset. We also manually removed sequences that corresponded with *Cholorplast* and *Mitochondria* as well as ambiguous and unclassified phylum annotations. DNA and RNA samples from each sampling date were treated as separate communities for all subsequent processing. ASVs with a prevalence lower than 5 reads in each sample were removed to avoid a small mean and trivially large coefficient of variation. Phantom taxa, defined as ASVs that were only observed in RNA and not in DNA [43], were also removed per sample. A total of 6 358 ASVs passed all filtration steps and were used in the subsequent biostatistical and community composition analyses. To account for data compositionality [58,59], centered log-ratio (clr) transformation and zero imputation were applied to the ASV count matrix using the cmultRepl function in the *zCompositions* (version 1.3.4) package based on geometric Bayesian multiplicative replacement and the clr function in the *compositions* package [60]. All statistical and model-based analyses were run using clr transformed ASV counts unless otherwise noted.

The six different particle size fractions were combined and analyzed in four size classes: <0.49 µm - the backup stage; 0.49 to 0.95 µm (stage 5) - fine fraction; 0.95 to 3.0 µm (stages 3-4) - intermediate fraction and 3.0 to 10.0 µm (stages 1-2) - coarse fraction. These subgroups correspond to bacterial cell debris (backup stage), single cells (fine fraction) and cell aggregates (coarse fraction). The intermediate size class is more likely to represent cell aggregates than single cells, as the cell diameter of a single bacterium is typically approximately 1 µm [61]. Due to the accumulation of cell debris and the bouncing effect on impactor stages [62], we excluded the backup stage (<0.49 µm) from further analysis.

Variance analysis (PERMANOVA) was conducted using the adonis2 function (1 000 permutations) in the *vegan* package [63] based on the Euclidean dissimilarity matrix. PERMANOVA models were run separately using the following designs: (1) for DNA and RNA communities, separately, the examined

variables were air-mass source, particle size and particle concentration, in this order, and (2) when separated by air-mass source, we examined the variance explained by sample type (RNA/DNA) and particle size class, in this order. For both cases, blocks were defined as sample dates to account for the nonindependence of different particle sizes sampled at the same time [64,65].

Richness (observed number of ASVs) and Shannon–Wiener diversity indices were calculated with the *Phyloseq* package [55]. The Kruskal–Wallis rank sum test and Wilcoxon signed-rank test were implemented for community richness, diversity and qPCR analyses using the *stats* R package. In the Wilcoxon signed-rank test, *p* values were adjusted for multiple testing using the Benjamini–Hochberg method [66].

ASVs that were significantly more abundant in the RNA community than in the DNA community were identified using a linear mixed model of the *MaAslin2* package [67]. The model was run separately for each air-mass source with the following design to examine associations between specific ASVs that are significantly more abundant in the RNA community and different particle size classes: *fixed effect = c (sample type, particle size), random effect = (sample date)*. The reference communities were defined as the DNA community and fine size class in the model. All reported *p* values were corrected using the Benjamini–Hochberg method [66], with results of $p < 0.05$ and adjusted $p < 0.2$ considered significant. Taxa that had a zero read count (raw count, before clr transformation) in DNA samples per air-mass source were excluded from the modeling result.

Results

Air-mass back trajectories and the potential origin of the dust

The sampling date, air-mass sources and PM_{10} concentrations are presented in Table 1. The air-mass back trajectories are also shown in Table S1. The air masses were classified into four groups considering the back trajectory analysis: NW, NE, SW and SE.

Air-mass origins, according to the calculated back trajectories, that coincided with high concentrations of suspended particulate matter in the dust column maps were assigned as the potential dust source. Air-mass sources classified as NE, SW and SE were associated with the three different main dust sources in the Eastern Mediterranean: Iraq and eastern Syria (NE), the Sahara Desert (SW) and the Arabian Peninsula (SE) [68]. Two of these sources, the Sahara Desert and the Arabian Peninsula, are among the world's largest dust sources, accounting for more than 50% of global dust emissions [69-71]. The air-mass source classified as NW was associated with low PM_{10} air masses with little to no contribution from the neighboring dust sources and thus represents mostly local airborne microorganisms.

Community-level multivariate comparison

Differences between the air-mass source, particle size class and PM_{10} concentration

Initially, we explored which of the different environmental parameters imposed a significant effect on the composition of the sampled airborne communities (both DNA and RNA). According to the PERMANOVA test, the dust source accounted for the highest ratio of variation for both DNA and RNA communities. When compared between the two, it was more pronounced in the RNA community (R^2 = 0.39, p < 0.001) than in the DNA community (R^2 = 0.24, p < 0.001). The PM_{10} concentrations for DNA and RNA had values of R^2 = 0.09 and 0.07 (p < 0.001), respectively. Finally, the particle size classes for DNA and RNA had values of R^2 = 0.06 and 0.04 (p < 0.001), respectively.

Differences between DNA and RNA within each air-mass source

To evaluate whether DNA and RNA communities significantly differed from each other as well as to assess the relative effect of particle size on the variability of bacterial communities, we separated communities according to the air-mass source and then performed a PERMANOVA significance test between the two communities, accounting for the particle size class. The results are presented in Table 2. According to the results, there was a significant difference between the DNA and RNA communities originating from the NE, SW and SE but not in those from the NW, possibly due to the high variance within these communities, along with the low number of samples from the NW. The effect of particle size was significant in the NE, SW and SE communities with similar ratios of variance (R^2 = 0.05-0.10, p = 0.025, 0.007 and 0.003) but not in those from the NW (p = 0.062), suggesting a great within-group similarity for different particle size classes in the NW communities.

Diversity and richness of DNA and RNA communities

Effect of the air-mass source

Alpha-diversity analyses, based on richness (observed number of ASVs) and Shannon–Wiener index of diversity, were conducted on DNA and RNA communities by air-mass source. The results are presented in Figure 1.

Similar patterns of richness and diversity between DNA and RNA of different air-mass sources were observed. According to a Kruskal–Wallis test, the source of the air mass significantly affected the diversity and richness of both the DNA and RNA communities (Kruskal–Wallis, p < 0.001). Specifically, according to a Wilcoxon signed-rank test, diversity and richness were significantly higher in air-mass samples that were associated with the dust sources (*i.e.*, NE, SW and SE) than those with NW trajectories. Both the richness and diversity of the RNA and DNA communities of the SE air masses were significantly higher than those of the SW air masses (Table 3).

We also compared the diversity and richness of the DNA and RNA communities of the same air-mass source. According to the Kruskal–Wallis test results, the diversity of DNA differed significantly from that of RNA (p = 0.009), but the observed richness did not (p = 0.429). Comparing the diversity of DNA vs. that of RNA in each air-mass source revealed no significant differences between the DNA and RNA diversity in the NE, SW and SE samples (Wilcoxon signed-rank test, p > 0.05). In the NW samples, the RNA community

diversity was significantly lower than the DNA community diversity ($p = 0.039$), possibly due to the high variance within the sources. All p values are presented in Table S2.

Effect of the particle-size class

When all the samples (*i.e.*, DNA and RNA) were divided by the particulate matter size classes (*i.e.*, fine, intermediate, and coarse), the diversity and richness differed significantly (Kruskal–Wallis, $p = 0.037$ and 0.003), as shown in Figure 1. Specifically, the richness of the coarse particle size class was significantly higher than that of the intermediate and fine particle size classes (Wilcoxon signed-rank test, $p = 0.038$ and $p = 0.007$). All p values are presented in Table S3.

Quantitative PCR

The qPCR results describe the number of 16S ribosomal RNA gene copies (DNA) and transcripts (RNA) per sampled m^3, as shown in Figure 2. Overall, the RNA concentrations were significantly higher than the DNA concentrations in all sources except those from the NW (NE $p = 0.024$; SW $p < 0.001$; SE $p = 0.001$; NW $p = 0.472$). In addition, the RNA concentrations were significantly higher than the DNA concentrations in the intermediate and coarse particle size classes ($p = 0.029$ and 0.040, respectively) but not in the fine size class ($p = 0.195$).

The RNA and DNA concentrations differed significantly between the different air-mass sources as well as between the particle size classes. According to Wilcoxon signed-rank tests, the DNA and RNA concentrations were higher in the NE ($p < 0.001$ and $p < 0.001$), SW ($p < 0.001$ and $p < 0.001$) and SE ($p < 0.001$ and $p < 0.001$) dust sources than those in the clear air masses from the NW; however, significant differences in the DNA and RNA concentrations were observed only among the airborne communities between SW and SE ($p = 0.020$ and $p = 0.005$, respectively), the latter with higher concentrations.

Bacterial taxa overrepresented in the RNA community

To identify potentially viable bacterial taxa that are significantly more abundant in the RNA community than in the DNA community, we applied a linear mixed model (MaAsLin2), as described in the methods section. The results are presented in Figure 3. Each chart represents clr-transformed mean values of DNA and RNA. Each dot represents a specific ASV. Significant results are colored according to phylum. The black line represents a slope of 1 and visually separates ASVs with higher (dots over the line) and lower (dots under the line) mean RNA abundance than the mean DNA abundance. We assumed that the ASVs that were overrepresented in the RNA community (*i.e.*, significantly high RNA abundance compared to DNA abundance) represented viable bacteria with a current protein synthesis potential [34]; hence, these taxa are more likely to ensure a rapid response in a new environment [72], whereas the ASVs overrepresented in the DNA community (*i.e.*, significantly high DNA abundance compared to RNA abundance) likely represented dead bacteria or relic DNA. The taxa that were significantly more abundant in the DNA and RNA communities were the source of variation between the two communities in each air-mass source. The ASVs that did not significantly differ between the RNA and DNA communities (*i.e.*,

denoted as “not significant” in Figure 3) represented taxa that were likely viable but, due to sampling and large variability in the population, were not identified as statistically significant in the model.

The number of ASVs that were overrepresented in the RNA community (MaAslin2, Benjamini–Hochberg adjusted $p < 0.2$) out of the total number of unique ASVs per air-mass source differed among the four air-mass sources: NW (152 of 1 249 ASVs), NE (307 of 3 388 ASVs), SW (2 438 of 4 164 ASVs) and SE (183 of 3 812 ASVs).

Proteobacteria and Firmicutes were the two dominant viable bacterial phyla (*i.e.*, with significantly high RNA abundance) despite evident differences between the different air-mass sources. While Proteobacteria was the most dominant phylum in the NW and NE samples, Firmicutes was the dominant phylum in the SE samples, and in the SW samples, Proteobacteria and Firmicutes were equally dominant. Actinobacteriota and Bacteroidota were the other two dominant phyla in all the air-mass sources but to a lesser extent.

At the family level, taxonomic differences were observed between the different sources; thus, Sphingomonadaceae, Rhodobacteraceae and Pseudomonadaceae were more common in the NW samples, whereas Sphingomonadaceae, Rhodobacteraceae, Hymenobacteraceae and Beijerinckiaceae dominated in the NE samples;
Lachnospiraceae, Sphingomonadaceae, Ruminococcaceae, Oscillospiraceae and Rhodobacteraceae dominated in the SW samples; and Lachnospiraceae, Ruminococcaceae, Rhodobacteraceae and Lactobacillaceae dominated in the SE samples. We did not find specific families dominated by dead ASVs (*i.e.*, with significantly high DNA abundance). All the significant ASVs and their taxonomic classifications are presented in Table S4.

Viable bacterial taxa associated with particle size classes

Furthermore, we evaluated the associations between viable bacterial taxa (*i.e.*, with significantly high RNA abundance) and the particle size classes. The results are presented in Figure 4. According to the results, 1 433 viable bacterial ASVs out of a total of 3 080 were associated with at least one of the particle size classes in all air-mass sources (MaAslin2, Benjamini–Hochberg adjusted $p < 0.2$). Many of these viable bacterial ASVs were associated with only the coarse particle size class (961 ASVs), followed by ASVs associated with both the intermediate and coarse size classes (369 ASVs) and then by the intermediate (89 ASVs) and fine (14 ASVs) size classes. Among the four different air-mass sources, more ASVs in the SW samples were found to be significantly associated with at least one of the particle size classes (1261 ASVs), followed by the NE (87 ASVs), NW (54 ASVs) and SE (31 ASVs) samples.

The viable bacterial families Bacteroidaceae, Hymenobacteraceae, Lachnospiraceae, Lactobacillaceae, Oscillospiraceae, Rhodobacteraceae, Ruminococcaceae and Sphingomonadaceae were associated with the coarse particle size class, while Acetobacteraceae, Micrococcaceae and Streptomycetaceae were associated with the fine particle size class.

Discussion

Factors influencing the community structure

This study was designed to extend our understanding of the factors that influence the community composition and structure of airborne bacteria, discerning between DNA (*i.e.*, dead and viable cells) and RNA (*i.e.*, viable cells only) communities, using a collection of samples representing various aerosol sources in a size-resolved manner. To the best of our knowledge, this is the first study implementing ribosomal DNA and RNA sequencing extracted from size-resolved aerosol samples, representing various air-mass sources, particle-size resolutions and PM_{10} concentrations.

The bacterial communities, as detected by 16S rRNA gene (DNA) and transcript (RNA) sequencing, varied in composition across all collected samples (Figure S1). This was in accordance with the observed diversity of the air-mass back trajectories. According to PERMANOVA, the air-mass source was the key variable responsible for the observed variance across all samples and the main environmental driver structuring the airborne community composition and assembly in both the DNA and RNA samples. This is consistent with findings in previous studies [4,6]. Particulate matter concentration and size class were the other two significant variables affecting the variance in airborne communities.

A higher proportion of total variance explained by the measured environmental variables (*i.e.*, air-mass source, particulate matter size class and concentrations) in RNA communities (R^2 = 0.50) than in DNA communities (R^2 = 0.39) suggests that viable bacteria better reflect environmental parameters than a collection of dead and viable members together (*i.e.*, the DNA community). Thus, DNA sequencing data alone may underestimate the effect of environmental parameters on microbial community composition. This may be expected since a cell's ribosomal RNA gene copy number per genome generally varies between 1 to 15 and is stable throughout the cell's lifetime unless a detrimental mutation occurs [73], whereas the number of transcripts synthesized per cell may reach up to thousands depending on the cellular metabolic state and nutrient availability [74-76].

The alpha diversity and richness of the NW samples were significantly lower than those of all other samples, suggesting that the communities coming from these sources are more diverse than those in the NW source. This is consistent with previous findings in previous studies at the same sampling location. These studies suggested that NW air masses, with a low PM_{10} concentration, are more likely to represent a local bacterial community [3,4,6].

Viable microorganisms represent the functional capacity to drive ecosystem processes. In bacteria, activity and growth are tightly regulated by ribosomal RNA transcription in accordance with the current physiological state of the cell and in response to changing environmental conditions [77-79]. However, there is not an absolute correlation between the concentration of RNA transcripts and the activity and growth of a cell. In fact, this relationship is likely to vary within and between different bacteria due to the different survival strategies [34]. Therefore, although the number of RNA transcripts per cell does not always

positively correlate with cell activity and growth, a high concentration of RNA transcripts indicates a specific taxon's current potential to rapidly respond to a new environment [72]. Relying on this assumption, we applied a comparative community analysis of 16S RNA and DNA using a linear mixed model in search of bacterial ASVs with significantly higher rRNA transcript abundance to identify viable aerial bacteria that are more likely to survive and drive ecosystem functions once they settle.

Dust-associated aerosols are rich in viable bacteria

According to our results, the RNA:DNA ratios (by qPCR) were between 1 and 86 (M = 10.43, SD = 12.99) in all samples, and only 2 696 ASVs (of 6 143 unique ASVs) were identified in the DNA and not in the RNA sequences from at least one of the four air-mass sources. This indicates that a significant portion of airborne bacteria are viable, whether during dust events or on clear days. To the best of our knowledge, this is the first comprehensive survey that quantifies the presence of viable bacteria in the atmosphere. Some previous studies investigated viable airborne bacteria by using culture-based methods and showed the presence of viable bacteria, some pathogenic, in the atmosphere [80,81]. According to our results, both DNA and RNA concentrations were significantly higher (Figure 2A) in transported dust (*i.e.*, NE, SW and SE) than in air masses representing local sources or long-range transport from Europe (*i.e.*, NW). This suggests that airborne bacteria can survive in the atmosphere for at least 3-4 days, and thus, the atmosphere is a significant dispersal pathway for viable bacteria [80,81]. These results further suggest that the local ecosystem in the receptor region is continuously subjected to a supply of active and diverse bacterial communities that are likely to compensate for the possible species loss caused by local anthropogenic activities.

The presence of significantly higher RNA transcript concentrations compared to DNA concentrations measured in collected dust samples (*i.e.*, NE, SW and SE) on coarse particles suggests that viable airborne bacteria are either attached to coarse particles or transported as cell aggregates. These results also indicate that bacteria transported attached to coarse particles or as aggregates are more likely to remain viable compared to bacteria attached to fine particles or to the probability of single cells surviving.

The similarity in DNA and RNA concentrations between the dust-borne communities (*i.e.*, NE, SW and SE samples) suggests that the air-mass source did not affect the viable and total amount of bacteria (*i.e.*, dead and viable cells together) carried on particulate matter as much as it affected the community composition, diversity and structure. This result also corroborates the conclusions of previous studies [3,4].

Viable atmospheric microbiome composition

The composition of viable communities varied between different air-mass sources, further corroborating previous results, indicating that different air masses are discernable by their bacterial community composition. Moreover, we have shown that some taxa have significantly higher transcript abundance than gene copy abundance, resulting in differences between DNA and RNA community composition per air-mass source, suggesting that biogeographic differences or varying harsh conditions during aerial transport may have a strong effect on the physiology of viable bacteria.

We identified multiple viable bacterial ASVs (*i.e.*, with significantly high RNA abundance), especially those that were the most dominant in each air-mass source, namely, *Lactobacillus*, *Paracoccus*, *Pseudomonas*, *Rubellimicrobium* and *Sphingomonas*, compositionally associated with the coarse particle size class, while very few ASVs of *Craurococcus-Caldovatus*, *Actinomycetospora*, *Actinophytocola*, *Micrococcus*, *Novosphingobium*, *Oceanobacillus*, *Streptomyces* and *Tianweitania* were associated with the fine size class, indicating that certain taxa may have a natural tendency to attach to coarse particles or be transported as cell aggregates.

Survival during aerial transport is challenged due to atmospheric conditions, such as desiccation, solar irradiation, and extreme temperatures, as well as extended periods with limited energy and nutrient sources. One survival strategy of microorganisms in harsh environments is through biofilm formation. A biofilm is a coordinated functional microbial community in which cells attach to each other and often to a surface, usually embedded into a self-produced matrix of extracellular polymeric substances (EPS) [82]. The viable bacterial ASVs associated with the coarse particle size class were the dominant taxa in all air masses. Among many others, *Lactobacillus*, *Paracoccus*, *Pseudomonas, Rubellimicrobium* and Sphingomonas are genera known to excrete exopolysaccharides [83-87]. EPS synthesis in atmospheric cloud microbial communities as a likely protection mechanism against harsh atmospheric conditions was also demonstrated by metagenomics and transcriptomics profiling of cloud water samples [18]. Therefore, the observation that multiple viable bacterial taxa are associated with the coarse particle size class may indicate that the innate tendency of the bacteria that attach to organic (*e.g.*, other bacteria) and inorganic particles (*e.g.*, mineral dust) or reside in cell aggregates is a significant factor in protecting them in the harsh conditions of their source environment (*i.e.*, deserts) and during atmospheric transport. Therefore, we presume that the dispersal of viable aerial bacterial communities may be less neutral [88] and that selective forces such as the coexistence of specific species and abiotic interactions with coarse particles are impactful in this process.

Interestingly, some of the viable bacterial taxa (*i.e.*, with significantly high RNA abundance), such as *Bacteroides*, *Christensenellaceae* R-7 group, *Lactobacillus*, *Rikenellaceae* RC9 gut group, *Roseomonas*, *Ruminococcus* torques group and UCG-005 (Family: Oscillospiraceae), are important commensal bacteria of the human and animal microbiomes, most of which are obligate anaerobes residing in the intestine [89-93]. Although it is not clear how anaerobic bacteria can be found viable in an aerobic environment (*i.e.*, atmosphere) at high abundance, we suggest that the possible transport of these taxa on dust particles or in cell aggregates is enveloped by biofilms possibly composed of exopolysaccharides, which can create a microanaerobic environment [94,95], enabling them to survive in the atmosphere. Although bacterial taxa of *Lactobacillus* and *Roseomonas* were reported to be a possible contaminant, especially in samples obtained from low-biomass environments [96], a higher ASV abundance of these taxa found in collected dust samples (*i.e.*, NE, SW and SE) compared to NW samples indicates that these bacteria were transported. Two species of the genus *Sphingomonas* (*i.e.*, *Sphingomonas paucimobilis* and *Sphingomonas suberifaciens*) are known human and plant pathogens, respectively [97-101]. The genus *Chryseobacterium* is another significant viable

bacterial taxon that was reported as an emerging potential multidrug-resistant human pathogen (*e.g.*, *Chryseobacterium indologenes*) [102]. This emphasizes the potential ecological impact of airborne viable bacteria, as these may be human, animal and plant pathogens.

Conclusions

It is often questioned whether the atmosphere can be an active ecosystem that can maintain Earth's biodiversity and support the transport of viable bacteria as well as human, animal, and plant pathogens. Several previous studies have suggested a continuous exchange of microorganisms between remote ecosystems, thus maintaining biodiversity and a healthy global ecosystem [22,103–105]. Our results show, for the first time, community composition data suggesting that airborne bacterial communities remain viable after long-range atmospheric transport. We found that the composition of the airborne viable bacterial communities from different locations varies with a diversified potential ecological impact. We suggest that the innate tendency of the bacteria to adhere to coarse particles or form cell aggregates is a significant factor in protecting bacteria in the harsh conditions of their source environment (*i.e.*, deserts) and during atmospheric transport and enables them to survive for 3–4 days in the atmosphere. Our results suggest that the atmosphere is a significant dispersal pathway for viable bacteria [80,81]. Although many of the viable bacteria that we identified are not reported to be harmful to human, animal, and plant health, their transport can suggest the potential atmospheric transport of pathogens that may pose public and environmental health risks both regionally and globally. Future studies will focus on the transport of viable pathogens to determine their potential effect.

Declarations

Data availability

Sequencing data are provided at the NCBI (SRA) database under the study accession code PRJNA765143 (https://www.ncbi.nlm.nih.gov/sra/PRJNA765143).

Acknowledgments

This study was partially supported by the Israel Science Foundation (grant 236/16), the Helmholtz Zentrum München and the Helmholtz Association (Berlin, Germany) in the framework of the AeroHEALTH Helmholtz International Lab (InterLabs-0005), a German-Israeli project. YR acknowledges support from a research grant from the Estate of Raymond Lapon and the Estate of Betty Weneser.

Competing Interests:

The authors declare no competing of interest.

References

1. Katra, I. *et al.* Richness and Diversity in Dust Stormborne Biomes at the Southeast Mediterranean. Scientific Reports **4**, 5265, doi:10.1038/srep05265 (2014).
2. Kellogg, C. A. & Griffin, D. W. Aerobiology and the global transport of desert dust. Trends in Ecology & Evolution **21**, 638–644, doi:https://doi.org/10.1016/j.tree.2006.07.004 (2006).
3. Mazar, Y., Cytryn, E., Erel, Y. & Rudich, Y. Effect of Dust Storms on the Atmospheric Microbiome in the Eastern Mediterranean. Environ Sci Technol **50**, 4194–4202, doi:10.1021/acs.est.5b06348 (2016).
4. Gat, D., Mazar, Y., Cytryn, E. & Rudich, Y. Origin-Dependent Variations in the Atmospheric Microbiome Community in Eastern Mediterranean Dust Storms. Environ Sci Technol **51**, 6709–6718, doi:10.1021/acs.est.7b00362 (2017).
5. Lang-Yona, N. *et al.* Links between airborne microbiome, meteorology, and chemical composition in northwestern Turkey. Science of The Total Environment **725**, 138227, doi:https://doi.org/10.1016/j.scitotenv.2020.138227 (2020).
6. Gat, D. *et al.* Size-Resolved Community Structure of Bacteria and Fungi Transported by Dust in the Middle East. Frontiers in Microbiology **12**, doi:10.3389/fmicb.2021.744117 (2021).
7. Hill, T. C. J. *et al.* Sources of organic ice nucleating particles in soils. Atmos. Chem. Phys. **16**, 7195–7211, doi:10.5194/acp-16-7195-2016 (2016).
8. Pandey, R. *et al.* Ice-nucleating bacteria control the order and dynamics of interfacial water. Sci Adv **2**, e1501630, doi:10.1126/sciadv.1501630 (2016).
9. Fröhlich-Nowoisky, J. *et al.* Ice nucleation activity in the widespread soil fungus < i > Mortierella alpina. Biogeosciences **12**, 1057–1071, doi:10.5194/bg-12-1057-2015 (2015).
10. Estillore, A. D., Trueblood, J. V. & Grassian, V. H. Atmospheric chemistry of bioaerosols: heterogeneous and multiphase reactions with atmospheric oxidants and other trace gases. Chemical Science **7**, 6604–6616, doi:10.1039/C6SC02353C (2016).
11. Brodie, E. L. *et al.* Urban aerosols harbor diverse and dynamic bacterial populations. *Proceedings of the National Academy of Sciences* **104**, 299–304, doi:10.1073/pnas.0608255104 (2007).
12. Šantl-Temkiv, T. *et al.* Characterization of airborne ice-nucleation-active bacteria and bacterial fragments. Atmospheric Environment **109**, 105–117, doi:https://doi.org/10.1016/j.atmosenv.2015.02.060 (2015).
13. Rahav, E., Ovadia, G., Paytan, A. & Herut, B. Contribution of airborne microbes to bacterial production and N2 fixation in seawater upon aerosol deposition. Geophysical Research Letters **43**, 719–727, doi:https://doi.org/10.1002/2015GL066898 (2016).
14. Failor, K. C., Schmale, D. G., Vinatzer, B. A. & Monteil, C. L. Ice nucleation active bacteria in precipitation are genetically diverse and nucleate ice by employing different mechanisms. The ISME Journal **11**, 2740–2753, doi:10.1038/ismej.2017.124 (2017).
15. de Araujo, G. G., Rodrigues, F., Gonçalves, F. L. T. & Galante, D. Survival and ice nucleation activity of Pseudomonas syringae strains exposed to simulated high-altitude atmospheric conditions. Scientific Reports **9**, 7768, doi:10.1038/s41598-019-44283-3 (2019).

16. Lazaridis, M. Bacteria as Cloud Condensation Nuclei (CCN) in the Atmosphere. Atmosphere **10**, 786 (2019).
17. Amato, P. *et al.* Active microorganisms thrive among extremely diverse communities in cloud water. PLOS ONE **12**, e0182869, doi:10.1371/journal.pone.0182869 (2017).
18. Amato, P. *et al.* Metatranscriptomic exploration of microbial functioning in clouds. Scientific Reports **9**, 4383, doi:10.1038/s41598-019-41032-4 (2019).
19. Vaïtilingom, M. *et al.* Potential impact of microbial activity on the oxidant capacity and organic carbon budget in clouds. *Proceedings of the National Academy of Sciences* **110**, 559–564, doi:10.1073/pnas.1205743110 (2013).
20. Triadó-Margarit, X., Cáliz, J. & Casamayor, E. O. A long-term atmospheric baseline for intercontinental exchange of airborne pathogens. Environment International **158**, 106916, doi:https://doi.org/10.1016/j.envint.2021.106916 (2022).
21. Brodie, E. L. *et al.* Urban aerosols harbor diverse and dynamic bacterial populations. *Proceedings of the National Academy of Sciences* **104**, 299, doi:10.1073/pnas.0608255104 (2007).
22. Archer, S. D. J. *et al.* Airborne microbial transport limitation to isolated Antarctic soil habitats. Nat Microbiol **4**, 925–932, doi:10.1038/s41564-019-0370-4 (2019).
23. Mayol, E. *et al.* Long-range transport of airborne microbes over the global tropical and subtropical ocean. Nature Communications **8**, 201, doi:10.1038/s41467-017-00110-9 (2017).
24. Favet, J. *et al.* Microbial hitchhikers on intercontinental dust: catching a lift in Chad. The ISME journal **7**, 850–867, doi:10.1038/ismej.2012.152 (2013).
25. Cáliz, J., Triadó-Margarit, X., Camarero, L. & Casamayor, E. O. A long-term survey unveils strong seasonal patterns in the airborne microbiome coupled to general and regional atmospheric circulations. *Proceedings of the National Academy of Sciences* **115**, 12229–12234, doi:10.1073/pnas.1812826115 (2018).
26. Du, P., Du, R., Ren, W., Lu, Z. & Fu, P. Seasonal variation characteristic of inhalable microbial communities in PM2.5 in Beijing city, China. Science of The Total Environment **610–611**, 308–315, doi:https://doi.org/10.1016/j.scitotenv.2017.07.097 (2018).
27. Lang-Yona, N. *et al.* Links between airborne microbiome, meteorology, and chemical composition in northwestern Turkey. Sci Total Environ **725**, 138227, doi:10.1016/j.scitotenv.2020.138227 (2020).
28. Gong, J., Qi, J., E, B., Yin, Y. & Gao, D. Concentration, viability and size distribution of bacteria in atmospheric bioaerosols under different types of pollution. Environmental Pollution **257**, 113485, doi:https://doi.org/10.1016/j.envpol.2019.113485 (2020).
29. Zhang, T., Li, X., Wang, M., Chen, H. & Yao, M. Time- and size-resolved bacterial aerosol dynamics in highly polluted air: new clues for haze formation mechanism. bioRxiv, 513093, doi:10.1101/513093 (2019).
30. Wei, M. *et al.* Size distribution of bioaerosols from biomass burning emissions: Characteristics of bacterial and fungal communities in submicron (PM1.0) and fine (PM2.5) particles. Ecotoxicology and Environmental Safety **171**, 37–46, doi:https://doi.org/10.1016/j.ecoenv.2018.12.026 (2019).

31. Richa, K. *et al.* Distribution, Community Composition, and Potential Metabolic Activity of Bacterioplankton in an Urbanized Mediterranean Sea Coastal Zone. Applied and Environmental Microbiology **83**, e00494-00417, doi:doi:10.1128/AEM.00494-17 (2017).
32. Damashek, J. *et al.* Transcriptional activity differentiates families of Marine Group II Euryarchaeota in the coastal ocean. ISME Communications **1**, 5, doi:10.1038/s43705-021-00002-6 (2021).
33. Hamilton, T. L., Peters, J. W., Skidmore, M. L. & Boyd, E. S. Molecular evidence for an active endogenous microbiome beneath glacial ice. The ISME Journal **7**, 1402–1412, doi:10.1038/ismej.2013.31 (2013).
34. Blazewicz, S. J., Barnard, R. L., Daly, R. A. & Firestone, M. K. Evaluating rRNA as an indicator of microbial activity in environmental communities: limitations and uses. Isme Journal **7**, 2061–2068, doi:10.1038/ismej.2013.102 (2013).
35. Barnard, R. L., Osborne, C. A. & Firestone, M. K. Responses of soil bacterial and fungal communities to extreme desiccation and rewetting. The ISME Journal **7**, 2229–2241, doi:10.1038/ismej.2013.104 (2013).
36. Schostag, M. *et al.* Distinct summer and winter bacterial communities in the active layer of Svalbard permafrost revealed by DNA- and RNA-based analyses. Frontiers in Microbiology **6**, doi:10.3389/fmicb.2015.00399 (2015).
37. Campbell, B. J., Yu, L., Heidelberg, J. F. & Kirchman, D. L. Activity of abundant and rare bacteria in a coastal ocean. *Proceedings of the National Academy of Sciences* **108**, 12776–12781, doi:10.1073/pnas.1101405108 (2011).
38. Denef, V. J., Fujimoto, M., Berry, M. A. & Schmidt, M. L. Seasonal Succession Leads to Habitat-Dependent Differentiation in Ribosomal RNA:DNA Ratios among Freshwater Lake Bacteria. Frontiers in Microbiology **7**, doi:10.3389/fmicb.2016.00606 (2016).
39. Zhang, Y., Zhao, Z., Dai, M., Jiao, N. & Herndl, G. J. Drivers shaping the diversity and biogeography of total and active bacterial communities in the South China Sea. Molecular Ecology **23**, 2260–2274, doi:https://doi.org/10.1111/mec.12739 (2014).
40. Hospodsky, D., Yamamoto, N. & Peccia, J. Accuracy, precision, and method detection limits of quantitative PCR for airborne bacteria and fungi. Appl Environ Microbiol **76**, 7004–7012, doi:10.1128/AEM.01240-10 (2010).
41. Nieto-Caballero, M., Savage, N., Keady, P. & Hernandez, M. High fidelity recovery of airborne microbial genetic materials by direct condensation capture into genomic preservatives. Journal of Microbiological Methods **157**, 1–3, doi:https://doi.org/10.1016/j.mimet.2018.12.010 (2019).
42. Behzad, H., Gojobori, T. & Mineta, K. Challenges and opportunities of airborne metagenomics. Genome Biol Evol **7**, 1216–1226, doi:10.1093/gbe/evv064 (2015).
43. Klein, A. M., Bohannan, B. J. M., Jaffe, D. A., Levin, D. A. & Green, J. L. Molecular Evidence for Metabolically Active Bacteria in the Atmosphere. Frontiers in microbiology **7**, 772–772, doi:10.3389/fmicb.2016.00772 (2016).

44. Amato, P. *et al.* Active microorganisms thrive among extremely diverse communities in cloud water. Plos One **12**, doi:ARTN e0182869 1371/journal.pone.0182869 (2017).
45. Vellend, B. M. Conceptual Synthesis in Community Ecology. The Quarterly Review of Biology **85**, 183–206, doi:10.1086/652373 (2010).
46. Krasnov, H., Katra, I. & Friger, M. Increase in dust storm related PM10 concentrations: A time series analysis of 2001–2015. Environ Pollut **213**, 36–42, doi:10.1016/j.envpol.2015.10.021 (2016).
47. Zittis, G., Hadjinicolaou, P., Fnais, M. & Lelieveld, J. Projected changes in heat wave characteristics in the eastern Mediterranean and the Middle East. Regional Environmental Change **16**, 1863–1876, doi:10.1007/s10113-014-0753-2 (2016).
48. Krasnov, H., Katra, I. & Friger, M. Increase in dust storm related PM10 concentrations: A time series analysis of 2001–2015. Environmental Pollution **213**, 36–42, doi:https://doi.org/10.1016/j.envpol.2015.10.021 (2016).
49. Stein, A. F. *et al.* Noaa's Hysplit Atmospheric Transport and Dispersion Modeling System. Bulletin of the American Meteorological Society **96**, 2059–2077, doi:10.1175/Bams-D-14-00110.1 (2015).
50. Rolph, G., Stein, A. & Stunder, B. Real-time Environmental Applications and Display sYstem: READY. Environmental Modelling & Software **95**, 210–228, doi:10.1016/j.envsoft.2017.06.025 (2017).
51. Acker, J. G. & Leptoukh, G. Online analysis enhances use of NASA Earth science data. Eos, Transactions American Geophysical Union **88**, 14–17, doi:https://doi.org/10.1029/2007EO020003 (2007).
52. Brauer, S. L. *et al.* Culturable Rhodobacter and Shewanella species are abundant in estuarine turbidity maxima of the Columbia River. Environmental Microbiology **13**, 589–603, doi:10.1111/j.1462-2920.2010.02360.x (2011).
53. Caporaso, J. G. *et al.* Ultra-high-throughput microbial community analysis on the Illumina HiSeq and MiSeq platforms. Isme Journal **6**, 1621–1624, doi:10.1038/ismej.2012.8 (2012).
54. Callahan, B. J. *et al.* DADA2: High-resolution sample inference from Illumina amplicon data. Nature Methods **13**, 581-+, doi:10.1038/Nmeth.3869 (2016).
55. McMurdie, P. J. & Holmes, S. phyloseq: An R Package for Reproducible Interactive Analysis and Graphics of Microbiome Census Data. Plos One **8**, doi:ARTN e61217 1371/journal.pone.0061217 (2013).
56. Quast, C. *et al.* The SILVA ribosomal RNA gene database project: improved data processing and web-based tools. Nucleic Acids Research **41**, D590-D596, doi:10.1093/nar/gks1219 (2013).
57. Davis, N. M., Proctor, D. M., Holmes, S. P., Relman, D. A. & Callahan, B. J. Simple statistical identification and removal of contaminant sequences in marker-gene and metagenomics data. Microbiome **6**, doi:ARTN 226 1186/s40168-018-0605-2 (2018).
58. Martin-Fernandez, J. A., Hron, K., Templ, M., Filzmoser, P. & Palarea-Albaladejo, J. Bayesian-multiplicative treatment of count zeros in compositional data sets. Statistical Modelling **15**, doi:10.1177/1471082x14535524 (2015).

59. Palarea-Albaladejo, J. & Martin-Fernandez, J. A. zCompositions - R Package for multivariate imputation of left-censored data under a compositional approach. Chemometrics and Intelligent Laboratory Systems **143**, 85–96, doi:10.1016/j.chemolab.2015.02.019 (2015).
60. van den Boogaart, K. G. & Tolosana-Delgado, R. “compositions”: A unified R package to analyze compositional data. Computers & Geosciences **34**, 320–338, doi:https://doi.org/10.1016/j.cageo.2006.11.017 (2008).
61. Amato, P. *et al.* in Microbiology of Aerosols 1–21 (2017).
62. Rao, A. K. & Whitby, K. T. Nonideal collection characteristics of single stage and cascade impactors. American Industrial Hygiene Association Journal **38**, 174–179, doi:10.1080/0002889778507933 (1977).
63. Jari Oksanen, F. G. B., Michael Friendly, Roeland Kindt, Pierre Legendre, Dan McGlinn, Peter R. Minchin, R. B. O'Hara, Gavin L. Simpson, Peter Solymos, M. Henry H. Stevens, Eduard Szoecs and Helene Wagner. vegan: Community Ecology Package. (2020).
64. Gilmour, S. G. in *Wiley StatsRef: Statistics Reference Online*.
65. Margolin, B. H. in *Wiley StatsRef: Statistics Reference Online*.
66. Benjamini, Y. & Hochberg, Y. Controlling the False Discovery Rate: A Practical and Powerful Approach to Multiple Testing. Journal of the Royal Statistical Society. Series B (Methodological) **57**, 289–300 (1995).
67. Mallick, H. *et al.* Multivariable association discovery in population-scale meta-omics studies. PLOS Computational Biology **17**, e1009442, doi:10.1371/journal.pcbi.1009442 (2021).
68. Bodenheimer, S., Lensky, I. M. & Dayan, U. Characterization of Eastern Mediterranean dust storms by area of origin; North Africa vs. Arabian Peninsula. Atmospheric Environment **198**, 158–165, doi:https://doi.org/10.1016/j.atmosenv.2018.10.034 (2019).
69. Klingmüller, K., Pozzer, A., Metzger, S., Stenchikov, G. L. & Lelieveld, J. Aerosol optical depth trend over the Middle East. Atmos. Chem. Phys. **16**, 5063–5073, doi:10.5194/acp-16-5063-2016 (2016).
70. Notaro, M., Alkolibi, F., Fadda, E. & Bakhrjy, F. Trajectory analysis of Saudi Arabian dust storms. Journal of Geophysical Research: Atmospheres **118**, 6028–6043, doi:https://doi.org/10.1002/jgrd.50346 (2013).
71. Tegen, I. & Schepanski, K. The global distribution of mineral dust. *IOP Conference Series: Earth and Environmental Science* **7**, 012001, doi:10.1088/1755-1307/7/1/012001 (2009).
72. Emerson, J. B. *et al.* Schrödinger’s microbes: Tools for distinguishing the living from the dead in microbial ecosystems. Microbiome **5**, 86, doi:10.1186/s40168-017-0285-3 (2017).
73. Klappenbach, J. A., Saxman, P. R., Cole, J. R. & Schmidt, T. M. rrndb: the Ribosomal RNA Operon Copy Number Database. Nucleic acids research **29**, 181–184, doi:10.1093/nar/29.1.181 (2001).
74. Bremer, H. & Dennis, P. P. Modulation of Chemical Composition and Other Parameters of the Cell at Different Exponential Growth Rates. EcoSal Plus **3**, doi:10.1128/ecosal.5.2.3 (2008).

75. Schneider, D. A., Ross, W. & Gourse, R. L. Control of rRNA expression in Escherichia coli. Curr Opin Microbiol **6**, 151–156, doi:10.1016/s1369-5274(03)00038-9 (2003).
76. Gralla, J. D. Escherichia coli ribosomal RNA transcription: regulatory roles for ppGpp, NTPs, architectural proteins and a polymerase-binding protein. Mol Microbiol **55**, 973–977, doi:10.1111/j.1365-2958.2004.04455.x (2005).
77. Davis, J. H. & Williamson, J. R. Structure and dynamics of bacterial ribosome biogenesis. Philos Trans R Soc Lond B Biol Sci **372**, doi:10.1098/rstb.2016.0181 (2017).
78. Maitra, A. & Dill, K. A. Bacterial growth laws reflect the evolutionary importance of energy efficiency. *Proceedings of the National Academy of Sciences* **112**, 406–411, doi:10.1073/pnas.1421138111 (2015).
79. Klumpp, S. & Hwa, T. Traffic patrol in the transcription of ribosomal RNA. RNA biology **6**, 392–394, doi:10.4161/rna.6.4.8952 (2009).
80. Hu, W. *et al.* Abundance and viability of particle-attached and free-floating bacteria in dusty and nondusty air. Biogeosciences **17**, 4477–4487, doi:10.5194/bg-17-4477-2020 (2020).
81. Griffin, D. W., Westphal, D. L. & Gray, M. A. Airborne microorganisms in the African desert dust corridor over the mid-Atlantic ridge, Ocean Drilling Program, Leg 209. *Aerobiologia* **22**, 211–226, doi:10.1007/s10453-006-9033-z (2006).
82. Yin, W., Wang, Y., Liu, L. & He, J. Biofilms: The Microbial "Protective Clothing" in Extreme Environments. International journal of molecular sciences **20**, 3423, doi:10.3390/ijms20143423 (2019).
83. Li, H. *et al.* The preparation and characterization of a novel sphingan WL from marine Sphingomonas sp. WG. Scientific Reports **6**, 37899, doi:10.1038/srep37899 (2016).
84. Riaz Rajoka, M. S., Wu, Y., Mehwish, H. M., Bansal, M. & Zhao, L. Lactobacillus exopolysaccharides: New perspectives on engineering strategies, physiochemical functions, and immunomodulatory effects on host health. Trends in Food Science & Technology **103**, 36–48, doi:https://doi.org/10.1016/j.tifs.2020.06.003 (2020).
85. Harrison, J. J. *et al.* Elevated exopolysaccharide levels in Pseudomonas aeruginosa flagellar mutants have implications for biofilm growth and chronic infections. PLOS Genetics **16**, e1008848, doi:10.1371/journal.pgen.1008848 (2020).
86. Raguénès, G. *et al.* A novel exopolymer-producing bacterium, Paracoccus zeaxanthinifaciens subsp. payriae, isolated from a "kopara" mat located in Rangiroa, an atoll of French Polynesia. Curr Microbiol **49**, 145–151, doi:10.1007/s00284-004-4303-x (2004).
87. Denner, E. B. M. *et al.* Rubellimicrobium thermophilum gen. nov., sp. nov., a red-pigmented, moderately thermophilic bacterium isolated from coloured slime deposits in paper machines. Int J Syst Evol Microbiol **56**, 1355–1362, doi:10.1099/ijs.0.63751-0 (2006).
88. Lowe, W. H. & McPeek, M. A. Is dispersal neutral? Trends in Ecology & Evolution **29**, 444–450, doi:https://doi.org/10.1016/j.tree.2014.05.009 (2014).

89. Zafar, H. & Saier, M. H., Jr. Gut Bacteroides species in health and disease. Gut Microbes **13**, 1–20, doi:10.1080/19490976.2020.1848158 (2021).
90. Walter, J. Ecological role of lactobacilli in the gastrointestinal tract: implications for fundamental and biomedical research. Appl Environ Microbiol **74**, 4985–4996, doi:10.1128/aem.00753-08 (2008).
91. Huang, C. *et al.* Microbiome and Metabolomics Reveal the Effects of Different Feeding Systems on the Growth and Ruminal Development of Yaks. Frontiers in Microbiology **12**, doi:10.3389/fmicb.2021.682989 (2021).
92. Schlappi, C. *et al.* Roseomonas gilardii Bacteremia in a Patient With HbSβ0-thalassemia: Clinical Implications and Literature Review. J Pediatr Hematol Oncol **42**, e385-e387, doi:10.1097/mph.0000000000001476 (2020).
93. Mancabelli, L. *et al.* Identification of universal gut microbial biomarkers of common human intestinal diseases by meta-analysis. FEMS Microbiology Ecology **93**, doi:10.1093/femsec/fix153 (2017).
94. Yoon, S. S. *et al.* Pseudomonas aeruginosa anaerobic respiration in biofilms: relationships to cystic fibrosis pathogenesis. Dev Cell **3**, 593–603, doi:10.1016/s1534-5807(02)00295-2 (2002).
95. Su, S. & Hassett, D. J. Anaerobic Pseudomonas aeruginosa and other obligately anaerobic bacterial biofilms growing in the thick airway mucus of chronically infected cystic fibrosis patients: an emerging paradigm or “Old Hat”? Expert Opinion on Therapeutic Targets **16**, 859–873, doi:10.1517/14728222.2012.708025 (2012).
96. Eisenhofer, R. *et al.* Contamination in Low Microbial Biomass Microbiome Studies: Issues and Recommendations. Trends in Microbiology **27**, 105–117, doi:https://doi.org/10.1016/j.tim.2018.11.003 (2019).
97. Ryan, M. P. & Adley, C. C. Sphingomonas paucimobilis: a persistent Gram-negative nosocomial infectious organism. J Hosp Infect **75**, 153–157, doi:10.1016/j.jhin.2010.03.007 (2010).
98. Souto, A., Guinda, M., Mera, A. & Pardo, F. Septic arthritis caused by Sphingomonas paucimobilis in an immunocompetent patient. Reumatol Clin **8**, 378–379, doi:10.1016/j.reuma.2012.06.002 (2012).
99. Lanoix, J. P. *et al.* Sphingomonas paucimobilis bacteremia related to intravenous human immunoglobulin injections. Med Mal Infect **42**, 37–39, doi:10.1016/j.medmal.2011.10.002 (2012).
100. van Bruggen, A. H., Brown, P. R. & Jochimsen, K. N. Corky root of lettuce caused by strains of a gram-negative bacterium from muck soils of Florida, new york, and wisconsin. Appl Environ Microbiol **55**, 2635–2640, doi:10.1128/aem.55.10.2635-2640.1989 (1989).
101. VAN BRUGGEN, A. H. C., JOCHIMSEN, K. N. & BROWN, P. R. Rhizomonas suberifaciens gen. nov., sp. nov., the Causal Agent of Corky Root of Lettuce. International Journal of Systematic and Evolutionary Microbiology **40**, 175–188, doi:https://doi.org/10.1099/00207713-40-2-175 (1990).
102. Izaguirre-Anariba, D. E. & Sivapalan, V. Chryseobacterium indologenes, an Emerging Bacteria: A Case Report and Review of Literature. Cureus **12**, e6720-e6720, doi:10.7759/cureus.6720 (2020).
103. Maki, T. *et al.* Aeolian Dispersal of Bacteria Associated With Desert Dust and Anthropogenic Particles Over Continental and Oceanic Surfaces. Journal of Geophysical Research: Atmospheres **124**, 5579–5588, doi:https://doi.org/10.1029/2018JD029597 (2019).

104. Šantl-Temkiv, T., Gosewinkel, U., Starnawski, P., Lever, M. & Finster, K. Aeolian dispersal of bacteria in southwest Greenland: their sources, abundance, diversity and physiological states. FEMS Microbiol Ecol **94**, doi:10.1093/femsec/fiy031 (2018).
105. Gonzalez-Martin, C., Teigell-Perez, N., Valladares, B. & Griffin, D. W. in *Advances in Agronomy* Vol. 127 (ed Donald Sparks) 1–41 (Academic Press, 2014).

Tables

Table 1. Sampling date, particulate matter source and concentration.

Date	Air-mass source	Mean PM_{10} ($\mu g \cdot m^{-3}$)
25.10.2019	Southwest	24.4 ± 7.8
26.10.2019	Southwest	37.8 ± 12.3
28.10.2019	Northwest	35.5 ± 5.1
10.11.2019	Northeast	74 ± 17.6*
13.11.2019	Southeast	98.8 ± 18.2*
14.11.2019	Southeast	66.7 ± 10.6*
18.11.2019	Northeast	60.7 ± 23.1*
26.11.2019	Southwest	119.9 ± 14.8*
11.12.2019	Southwest	33.9 ± 4.3
11.6.2020	Northwest	32.8 ± 6.5
24.06.2020	Northwest	35.1 ± 10.8
28.07.2020	Northwest	35.5 ± 13.3

PM_{10} values represent the mean daily concentration of particulate matter measuring 10 µm or less in diameter on each sampling date. The mean values corresponding to a high PM10 concentration (*i.e.*, dusty days) represented by an asterisk (*) symbol. The data were obtained from and are available at http://www.svivaaqm.net.

Table 2. PERMANOVA significance test between the two communities (*i.e.*, DNA/RNA) and different particle size classes (*i.e.*, fine, intermediate and coarse) separated according to the air-mass source. Significant *p*values are underlined.

	Northwest		Northeast		Southwest		Southeast	
Variable	R^2	*p* value	R^2	*p* value	R^2	*p* value	R^2	*p* value
DNA/RNA	0.11	0.948	0.05	0.049	0.09	< 0.001	0.06	0.005
Particle	0.06	0.062	0.10	0.025	0.05	0.007	0.10	0.003

Table 3. Significance of differences (Wilcoxon signed-rank test) in diversity and richness between airborne communities based on sampled DNA and RNA. Significant *p* values are underlined.

Sources compared	*p* values			
	Shannon–Wiener diversity		Observed richness	
	DNA	RNA	DNA	RNA
NW - NE	0.003	0.001	0.032	0.001
NW - SW	0.002	0.001	0.014	0.001
NW - SE	0.002	0.001	0.002	0.001
NE - SW	0.065	0.213	0.312	1.000
NE - SE	0.623	0.384	0.105	0.040
SW - SE	0.001	0.003	0.001	0.001

Figures

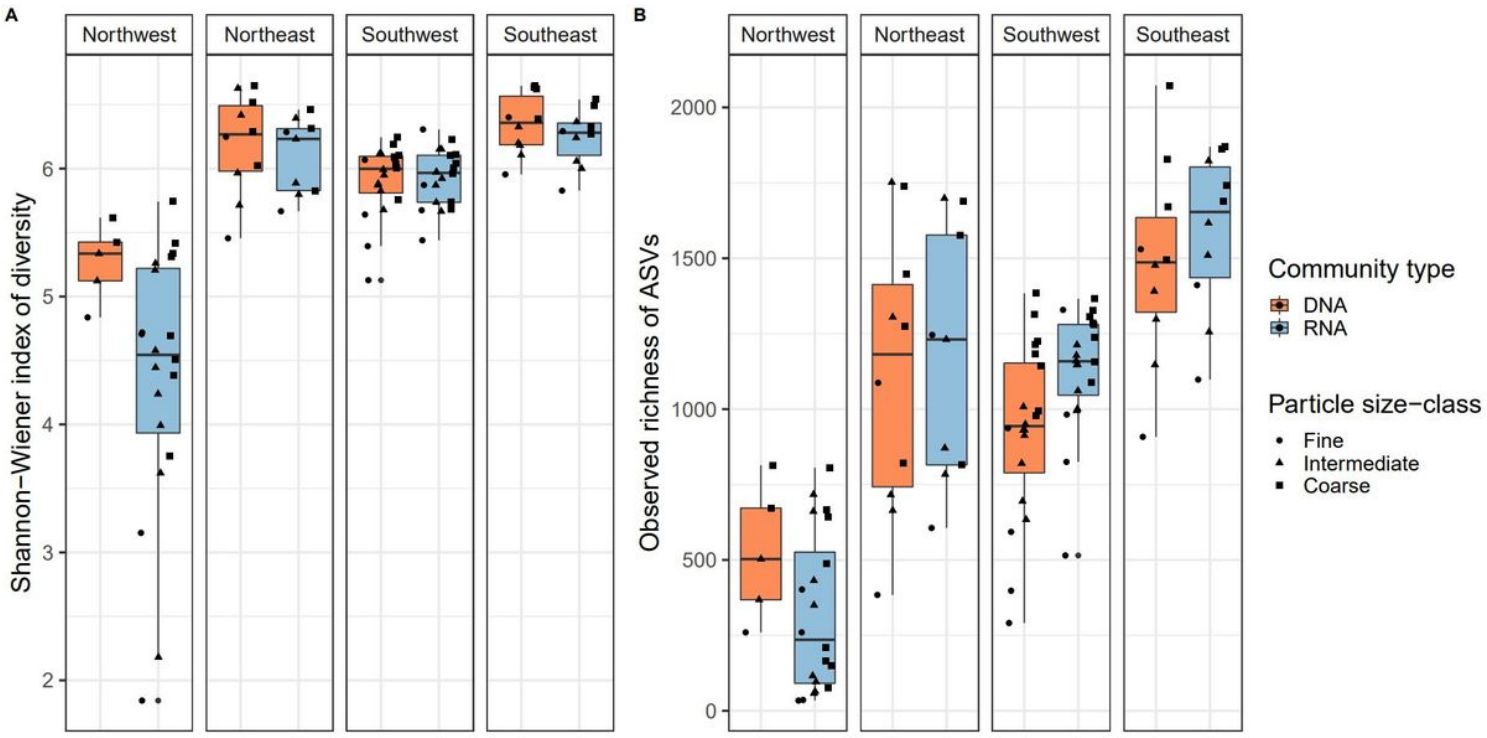

Figure 1

Shannon–Wiener diversity indices (A) and observed richness (B) within DNA and RNA communities of different air-mass sources. Community type and particle size classes are represented by different colors and symbol shapes, respectively, in each air-mass community. Boxes represent the interquartile range (IQR of 1.5), the line within the boxes is the median, and dots represent individual samples within each group.

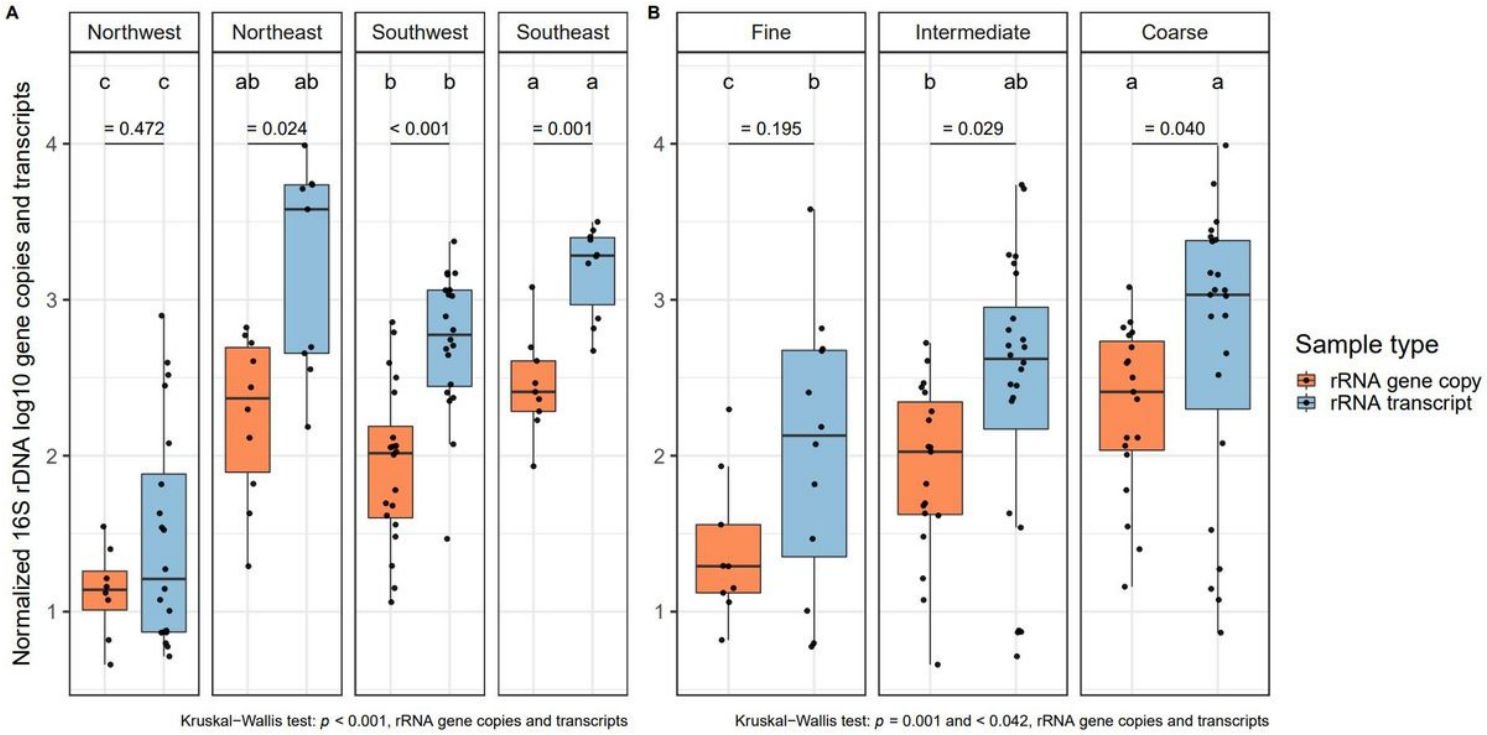

Figure 2

Total bacterial SSU rRNA gene copy and transcript concentrations of different (A) air-mass sources and (B) particulate matter size classes. The box plots show the normalized, log10 transformed number of bacterial SSU rRNA gene copies and transcripts per m^3 of sampled air. Boxes represent the interquartile range (IQR of 1.5), the line within the boxes is the median, and dots represent individual samples within each group. Lowercase letters indicate significant differences ($p < 0.05$) between the air-mass sources for gene copy and transcript concentrations, separately. *p* values of significance between gene copies and transcripts in each air-mass source and particle size class are also shown in each chart.

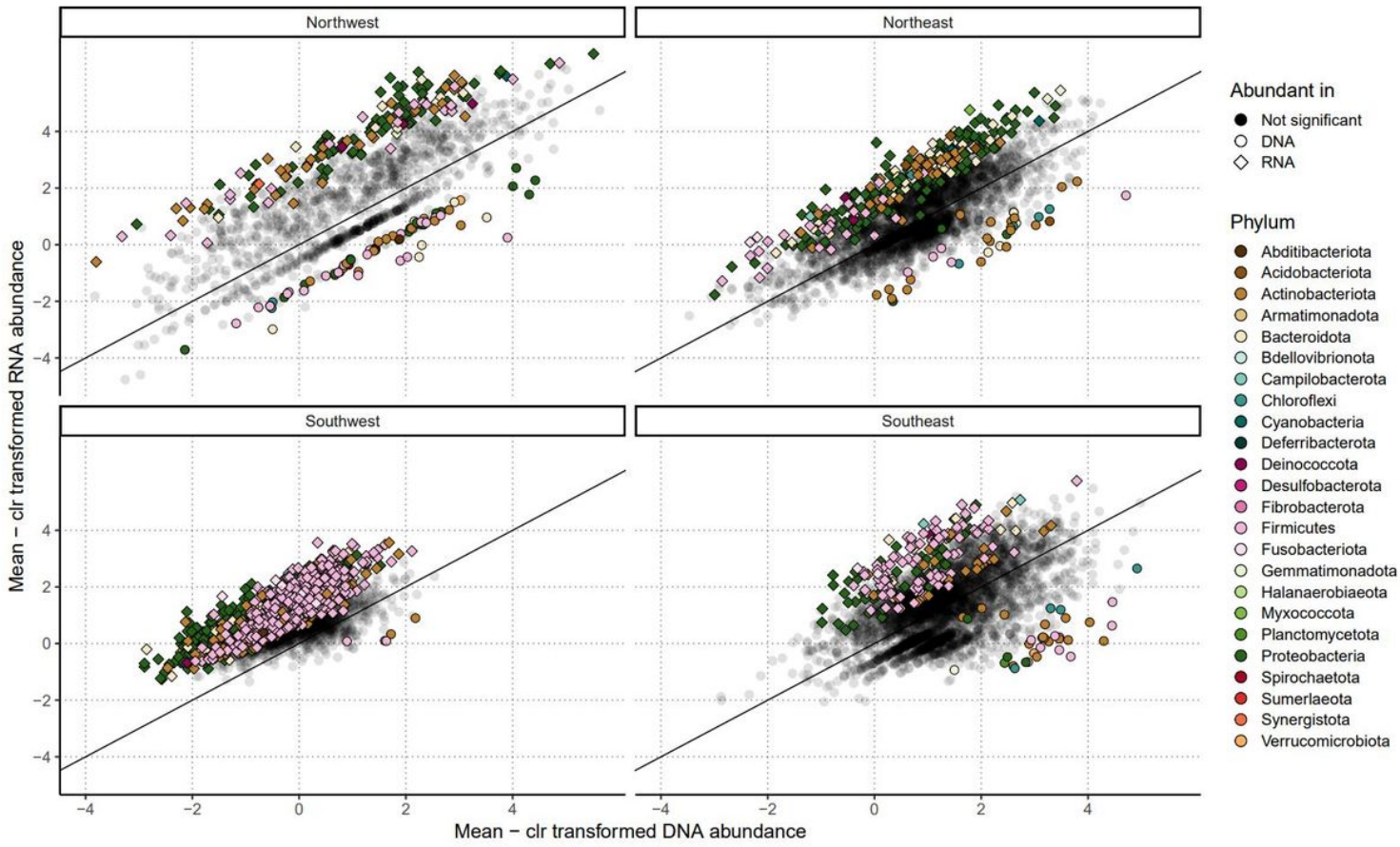

Figure 3

ASV mean abundance (represented by clr-transformed counts) in RNA (vertical axis) or DNA (horizontal axis) in each air-mass source. Significant results (MaAslin2, Benjamini–Hochberg adjusted $p < 0.2$) for ASVs overrepresented in the RNA community are depicted by colored dots, whereas ASVs overrepresented in the DNA community are shown as colored diamonds; each color represents a different phylum. The diagonal line represents a 1:1 ratio between RNA to DNA abundance. The full model results are also shown in Table S5.

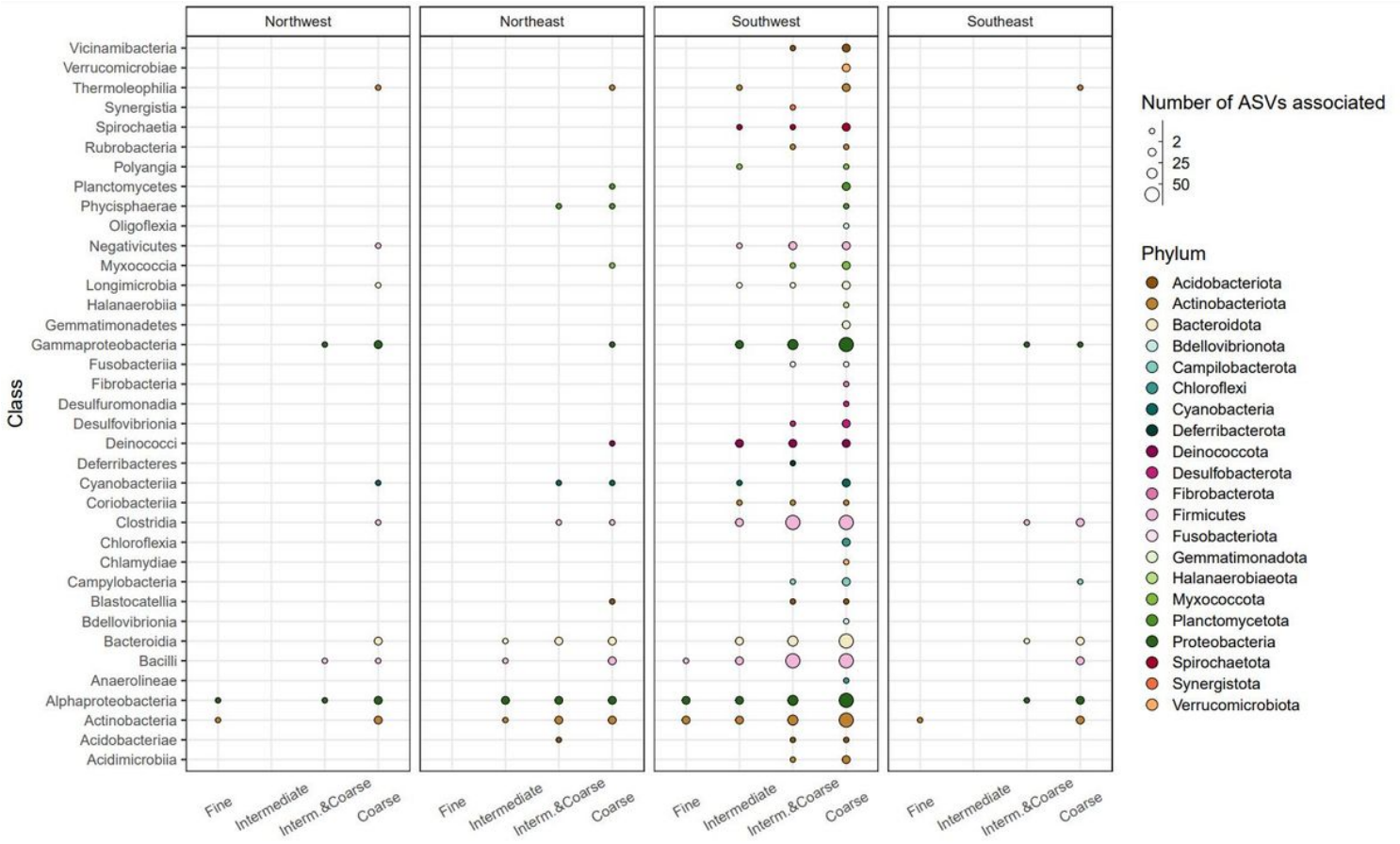

Figure 4

Viable bacterial ASVs (*i.e.*, with significantly high RNA abundance) associated with at least one of the particle size classes (MaAslin2, Benjamini–Hochberg adjusted $p < 0.2$). The y-axis represents phylum level taxonomic classification, whereas the x-axis shows the association with particle size class in each air-mass source. The number of ASVs associated with a specific particle size class is represented by the symbol size, while each color represents a different phylum. The full model results are also shown in Table S5.

Supplementary Files

This is a list of supplementary files associated with this preprint. Click to download.

- MovieS1theSouthwest25102019.avi
- MovieS2theSouthwest26102019.avi
- MovieS3theNorthwest28102019.avi
- MovieS4theNortheast10112019.avi
- MovieS5theSoutheast13112019.avi

- MovieS6theSoutheast14112019.avi
- MovieS7theNortheast18112019.avi
- MovieS8theSouthwest26112019.avi
- MovieS9theSouthwest11122019.avi
- MovieS10theNorthwest11062020.avi
- MovieS11theNorthwest24062020.avi
- MovieS12theNorthwest28072020.avi
- ErkorkmazetalSupplement.pdf
- TableS4.xlsx
- TableS5.xlsx